

A New Anharmonic Factor and EXAFS Including Anharmonic Contributions

Nguyen Van HUNG*, Nguyen Ba DUC[†] and Ronald R. FRAHM[‡]

Bergische Universitaet-Gesamthochschule Wuppertal, FB: 8-Physik, Gauss-Strasse 20, 42097 Wuppertal, Germany

(Received October 25, 2002)

A new anharmonic factor and the extended X-ray absorption fine structure (EXAFS) including anharmonic contributions have been developed based on the cumulant expansion and the single-shell model. Analytical expressions for the anharmonic contributions to the amplitude and to the phase of the EXAFS have been derived. The EXAFS and its parameters contain anharmonic effects at high temperature and approach those of the harmonic model at low temperature. Numerical results for Cu agree well with experiment. Peaks in the Fourier transform of the calculated anharmonic EXAFS for the first shell at 297 K and 703 K agree well with the experimental ones and are shifted significantly compared to those of the harmonic model.

KEYWORDS: anharmonic EXAFS, cumulants, temperature dependence
DOI: 10.1143/JPSJ.72.1254

1. Introduction

The harmonic approximation in EXAFS calculations works very well¹⁾ at low temperatures because the anharmonic contributions to atomic thermal vibrations can be neglected. But at different high temperatures the EXAFS spectra provide apparently different structural information^{2–17)} due to the anharmonicity, and these effects need to be evaluated. Moreover, for some aspects like catalysis research the EXAFS studies carried out at low temperature may not provide a correct structural picture and the high-temperature EXAFS, where the anharmonicity must be included, is necessary.²⁾ The formalism for including anharmonic effects in EXAFS is often based on the cumulant expansion approach,^{3,5)} according to which the EXAFS oscillation function is described by

$$\chi(k) = F(k) \frac{e^{-2R/\lambda(k)}}{kR^2} \text{Im} \left\{ e^{i\Phi(k)} \exp \left[2ikR + \sum_n \frac{(2ik)^n}{n!} \sigma^{(n)} \right] \right\} \quad (1)$$

where $F(k)$ is the real atomic backscattering amplitude, Φ is the net phase shift, k and λ are the wave number and the mean free path of the photoelectron, respectively, and $\sigma^{(n)}$ ($n = 1, 2, 3, \dots$) are the cumulants. They appear due to the thermal average of the function $\exp(i2kr)$ in which the asymmetric terms are expanded in a Taylor series about $R = \langle r \rangle$ with r as the instantaneous bond length between absorbing and backscattering atoms and then are rewritten in terms of cumulants.

Based on this approach the anharmonic effects in EXAFS have been often valued by the ratio methods.^{3–9)} Another way is the direct calculation and analysis of EXAFS and its parameters including anharmonic effects at any temperature. For this purpose an anharmonic factor has been introduced^{10–12)} to take into account the anharmonic contributions to the mean square relative displacement (MSRD). This procedure provides a good agreement with experiment,¹¹⁾ but the expressions for the anharmonic factor and

for the phase change of the EXAFS due to anharmonicity contain a fitting parameter, and the cumulants were obtained by an extrapolation procedure from the experimental data.

This work firstly is a next step of ref. 11 to develop an analytical procedure which overcomes the above mentioned limitations and to show more information. Our further development is the derivation of analytical expressions for the anharmonic factor determining the anharmonic contributions to the amplitude and for the anharmonic contributions to the phase of the EXAFS. The cumulants contained in the derived expressions can be considered by several procedures.^{4,6,7,13–16)} In this work the quantum statistical approach with anharmonic correlated Einstein model¹⁵⁾ has been used for calculation of the cumulants in which the parameters of the anharmonic effective potential are based on a Morse potential that characterizes the interaction between each pair of atoms. Including contributions of all atoms in all directions in a small cluster by a simple way¹⁵⁾ this model avoids full lattices dynamical¹⁴⁾ or dynamical matrix¹⁶⁾ calculations jet provides reasonable agreement with experiment and with the other theory results¹⁴⁾ even for the case of strongly anharmonic crystal Cu. This model also is successful in extracting physical parameters from the EXAFS measured data,²⁷⁾ as well as in the investigation of local force constants of transition metal dopants in a Nickel host,²⁸⁾ and in contribution to theoretical approaches to the EXAFS.²⁹⁾ Moreover, for nanostructure the clusters become too small the bulk theory may start to break down, which is one place the small cluster approach¹⁵⁾ input is necessary.²⁹⁾ This work secondly is a next step of the work by Hung and Rehr¹⁵⁾ applying the anharmonic correlated Einstein model to calculation and analysis of EXAFS and its parameters including anharmonic contributions. We get the total MSRD and the EXAFS function which include anharmonic effects at high temperatures and are approaching those of the harmonic model at low temperatures. Cu metal spectra, which are often used for testing new theories^{2,11,14,15,18,27)} also have been considered in this work, and numerical results are found to be in good agreement with experiment.^{17,19)}

*E-mail: vhung@phys-hu.edu.vn

[†]Permanent address: Department of Physics, Hanoi National University, 334 NguyenTrai, Hanoi, Vietnam. E-mail: nbduc@netnam.vn

[‡]E-mail: frahm@uni-wuppertal.de

2. Formalism

The EXAFS oscillation function eq. (1) including anharmonic effects contains the Debye–Waller factor $e^{-W(k,T)}$ accounting for the effects of the thermal vibrations of atoms. Based on the analysis^{4,15)} of cumulant expansion we obtain

$$W(k, T) = 2ik\sigma^{(1)}(T) - 2k^2\sigma^{(2)}(T) - 4ik\sigma^{(2)}(T)\left(\frac{1}{R} - \frac{1}{\lambda(k)}\right) - \frac{4}{3}ik^3\sigma^{(3)}(T) + \frac{2}{3}\sigma^{(4)}(T)k^4 + \dots, \quad (2)$$

where $\sigma^{(1)}$ is the first cumulant or net thermal expansion, $\sigma^{(2)}$ is the second cumulant which is equal to the MSRD σ^2 , $\sigma^{(3)}$ and $\sigma^{(4)}$ are the third and the fourth cumulants, respectively, the remaining parameters were defined above. The higher cumulants are not included due to their small contributions.^{3,5)}

To consider anharmonic contributions to the MSRD we used an argument analogous to the one²⁰⁾ for its change due to the temperature increase and obtain

$$\sigma^2(T) - \sigma^2(T_0) = (1 + \beta(T))[\sigma_H^2 - \sigma^2(T_0)]; \quad (3)$$

$$\beta(T) = 2\gamma_G \frac{\Delta V}{V}$$

where γ_G is Grüneisen parameter, and $\Delta V/V$ is the relative volume change due to thermal expansion, T_0 is a very low temperature so that $\sigma^2(T_0)$ is a harmonic MSRD. This result agrees with the one in another consideration⁴⁾ on the change of the MSRD. Developing further eq. (3) we obtain the total MSRD

$$\sigma^2(T) = \sigma_H^2(T) + \beta(T)[\sigma_H^2 - \sigma^2(T_0)], \quad (4)$$

It is clear that the MSRD approaches the very small value of zero-point contribution σ_0^2 when the temperature approaches zero, i.e.,

$$\sigma^2(T_0) \rightarrow \sigma_0^2, \quad \text{for } T_0 \rightarrow 0.$$

Hence, it can be seen in eq. (4) that the total MSRD $\sigma^2(T)$ at a given temperature T consists of the harmonic contribution $\sigma_H^2(T)$ and the anharmonic one $\sigma_A^2(T)$

$$\sigma^2(T) = \sigma_H^2(T) + \sigma_A^2(T); \quad \sigma_A^2(T) = \beta(T)[\sigma_H^2(T) - \sigma_0^2], \quad (5)$$

This separation will help us to determine the anharmonic contribution to the EXAFS amplitude.

We will illustrate the theory for a simple fcc crystal, though the generalization to other structures or longer-range interactions is straightforward. In the present approach we apply the anharmonic correlated Einstein model¹⁵⁾ to the calculation of cumulants where the effective potential is given by

$$V_{\text{eff}}(x) \cong \frac{1}{2}k_{\text{eff}}x^2 + k_3x^3 + \dots$$

$$= V(x) + \sum_{j \neq i} V\left(\frac{\mu}{M_i}x\hat{\mathbf{R}}_{12}, \hat{\mathbf{R}}_{ij}\right), \quad \mu = \frac{M_1M_2}{M_1 + M_2}. \quad (6)$$

Here x is the deviation of instantaneous bond length between two atoms from equilibrium, $\hat{\mathbf{R}}$ is the bond unit vector, k_{eff} is

effective spring constant, and k_3 the cubic parameter giving an asymmetry in the pair distribution function. The correlated Einstein model may be defined as a oscillation of a pair of atoms with masses M_1 and M_2 (e.g., absorber and backscatterer) in a given system. The contributions of all their neighbors in all directions in a small cluster are given by the last term in the left-hand side of eq. (6), where the sum i is over absorber ($i = 1$) and backscatterer ($i = 2$), and the sum j is over all their near neighbors, excluding the absorber and backscatterer themselves whose contributions are described by the term $V(x)$.

To model the asymmetry we replaced the harmonic potential by an anharmonic one, e.g., a Morse potential²¹⁾ with parameters D and α which characterizes the interaction of each pair of atoms. Applying it to the effective potential of the system of eq. (6) (ignoring the overall constant) we obtain

$$k_{\text{eff}} = 5D\alpha^2\left(1 - \frac{3}{2}\alpha a\right) = \mu\omega_E^2; \quad (7)$$

$$k_3 = -\frac{5}{4}D\alpha^3; \quad \theta_E = \frac{\hbar\omega_E}{k_B},$$

where k_B is the Boltzmann constant; ω_E, θ_E are the correlated Einstein frequency and temperature.

Using the above results in first-order thermodynamic perturbation theory^{13,15)} with consideration of the phonon–phonon interaction for taking into account the anharmonicity we obtain the cumulants

$$\sigma^{(1)}(T) = a(T) = \sigma_0^{(1)}\frac{1+z}{1-z}; \quad \sigma_0^{(1)} = \frac{3\alpha}{4}\sigma_0^{(2)} \quad (8)$$

$$\sigma^2(T) = \sigma_0^2\frac{1+z}{1-z}; \quad \sigma_0^2 = \frac{\hbar\omega_E}{10D\alpha^2}, \quad z = e^{-\theta_E/T} \quad (9)$$

$$\sigma^{(3)}(T) = \sigma_0^{(3)}(T)\frac{1+10z+z^2}{(1-z)^2}; \quad \sigma_0^{(3)} = \frac{\alpha}{2}(\sigma_0^{(2)})^2, \quad (10)$$

where $\sigma_0^{(1)}, \sigma_0^{(2)}, \sigma_0^{(3)}$ are the zero-point contributions to the first, second and third cumulant, respectively.

We calculated the relative thermal volume change $\Delta V/V$ using $R(T) = R + a(T)$ and Grüneisen parameter $\gamma_G = -\frac{\partial \ln \omega_E}{\partial \ln V}$. By substituting the obtained results in eq. (3) we derived an anharmonic factor

$$\beta(T) = \frac{9\eta(T)k_B T}{16D}\left[1 + \frac{3k_B T}{8DR\alpha}\left(1 + \frac{3k_B T}{8DR\alpha}\right)\right]; \quad (11)$$

$$\eta(T) = \frac{2e^{-\theta_E/T}}{1 + e^{-\theta_E/T}}.$$

This factor is proportional to the temperature and inversely proportional to the shell radius, thus reflecting a similar property of anharmonicity obtained in an experimental catalysis research²⁾ if R is considered as particle radius.

The anharmonic contribution Φ_A to the EXAFS phase at a given temperature is the difference between the total phase and the one of the harmonic EXAFS. On the left-hand side of eq. (2) the 2nd and the 5th terms contribute to the EXAFS amplitude. Only the 1st, the 4th terms and the anharmonic contributions to the MSRD in the 3rd term are the anharmonic contributions to the phase. Therefore, from this equation we obtain

$$\phi_A(T, k) = 2k \left[\sigma^{(1)}(T) - 2\sigma_A^2(T) \left(\frac{1}{R} - \frac{1}{\lambda(k)} \right) - \frac{2}{3} \sigma^{(3)}(T) k^2 \right]. \quad (12)$$

$$\chi(k, T) = \sum_j \frac{S_0^2 N_j}{k R_j^2} F_j(k) e^{-(2k^2 \sigma^2(T) + 2R_j/\lambda(k))} \sin(2kR_j + \phi_j(k) + \phi_A^j(k, T)) \quad (13)$$

which by taking eq. (5) into account is resulting in

$$\chi(k, T) = \sum_j \frac{S_0^2 N_j}{k R_j^2} F_j(k) e^{-(2k^2 [\sigma_{\text{h}}^2(T) + \sigma_A^2(T)] + 2R_j/\lambda(k))} \sin(2kR_j + \phi_j(k) + \phi_A^j(k, T)) \quad (14)$$

where S_0^2 is the square of the many body overlap term, N_j is the atomic number of each shell, the remaining parameters were defined above, the mean free path λ is defined by the imaginary part of the complex photoelectron momentum $p = k + i/\lambda$, and the sum is over all atomic shells.

It is obvious that in eq. (14) $\sigma_A^2(T)$ determines the anharmonic contribution to the amplitude characterizing the attenuation, and $\Phi_A(k, T)$ is the anharmonic contribution to the phase characterizing the phase shift of EXAFS spectra. They are calculated by eqs. (5) and (12), respectively. Their values characterize the temperature dependence of the anharmonicity, but the anharmonicity is described by the cumulants given by eqs. (8)–(10) obtained by consideration of the phonon–phonon interaction process. That is why they also characterize the temperature dependence of the phonon–phonon interaction in the EXAFS theory. At low temperatures these anharmonic values approach zero and the EXAFS function eq. (14) is reduced to the one of the harmonic model.

The Morse potential parameters D and α can be obtained using experimental values of the energy of sublimation, the compressibility, and the lattice constant, which are known already.²²⁾ A such method for calculation of the Morse potential parameters has been developed for cubic crystals²³⁾ and for other structures.²⁴⁾

3. Discussion of Numerical Results and Comparison with Experiment

We applied the expressions derived in the previous section to numerical calculations for Cu, Al, and Ni. Their Morse potential parameters²³⁾ D , α ; calculated effective spring constant k_{eff} , correlated Einstein frequency ω_E and temperature θ_E are written in Table I, where our calculated value $\theta_E \approx 236$ K for Cu agrees well with the measured one of 232(5) K.⁹⁾ Figure 1 shows the temperature dependence of our calculated anharmonic factors $\beta(T)$ for Cu, Al and Ni. In the case of Cu it has the values 0.028 at 300 K and 0.084 at 700 K which agree well with those obtained in the other studies.^{11,25)} Figure 2 shows the temperature dependence of our calculated anharmonic contribution $\sigma_A^2(T)$ to the MSRD determining the anharmonic contribution to the EXAFS amplitude of Cu. It is small at low temperatures and then increases strongly at high temperatures having a form looking like the one of the third cumulant (Fig. 5). This result also shows that below 100 K no anharmonic effect in the EXAFS of Cu is expected. It agrees well with our

The 4th cumulant is often very small.^{13,15,17)} This is why we obtained from eqs. (1) and (2), taking into account the above results, the temperature dependent K-edge EXAFS function including anharmonic effects as

Table I. Morse potential parameters D , α , the calculated effective spring constant k_{eff} , correlated Einstein frequency ω_E , Einstein temperature θ_E of Cu, Al and Ni.

Crystal	D (eV)	α (\AA^{-1})	k_{eff} (N/m)	ω_E (10^{13} Hz)	θ_E (K)
Cu	0.3429	1.3588	50.7478	3.0889	235.9494
Al	0.2703	1.1646	29.3686	3.6102	275.7695
Ni	0.4205	1.4149	67.9150	3.7217	284.3095

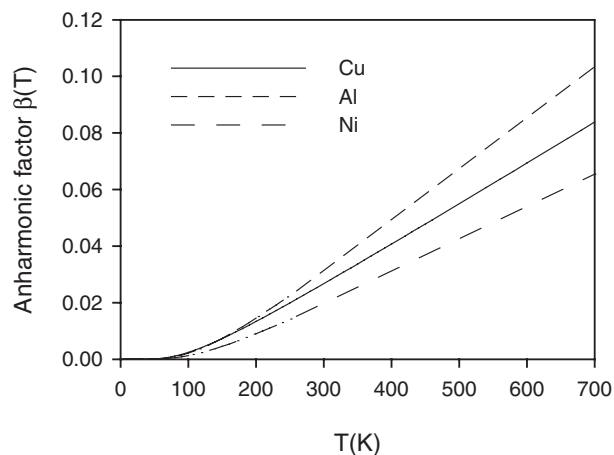


Fig. 1. Temperature dependence of the calculated anharmonic factor $\beta(T)$ for Cu, Al and Ni.

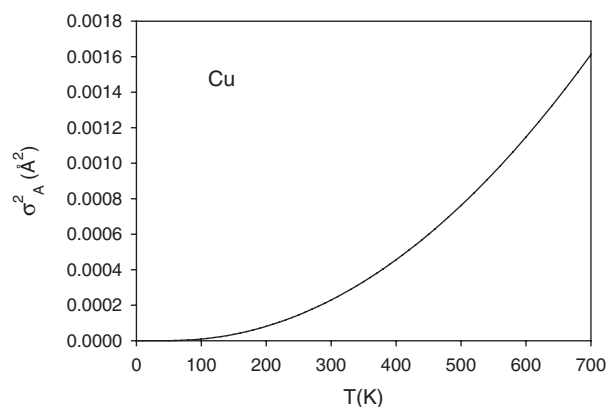


Fig. 2. Temperature dependence of the calculated anharmonic contribution $\sigma_A^2(T)$ to the MSRD determining the anharmonic contributions to the EXAFS amplitude.

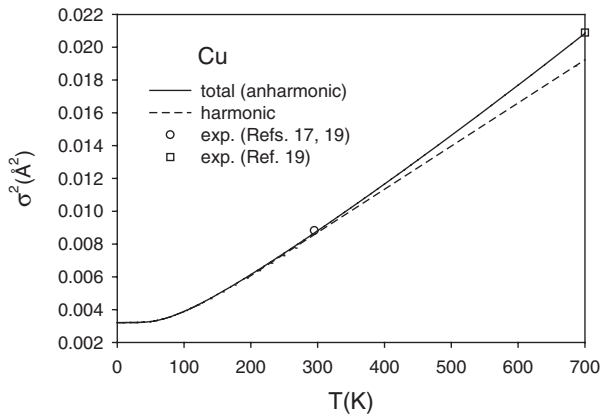


Fig. 3. Temperature dependence of the calculated total MSRD $\sigma^2(T)$ of Cu compared to the harmonic one $\sigma_H^2(T)$ and to the measured values at 295 K^{17,19)} and at 700 K.¹⁹⁾

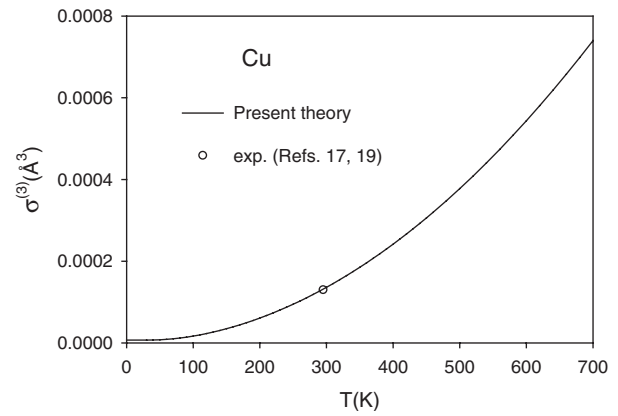


Fig. 5. Temperature dependence of the calculated third cumulant $\sigma^{(3)}(T)$ of Cu compared to the measured value at 295 K.^{17,19)}

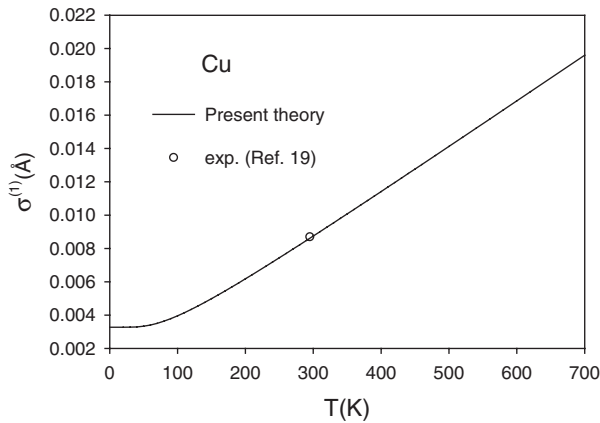


Fig. 4. Temperature dependence of the calculated first cumulant $\sigma^{(1)}(T)$ or net thermal expansion of Cu compared to the measured value at 295 K.¹⁹⁾

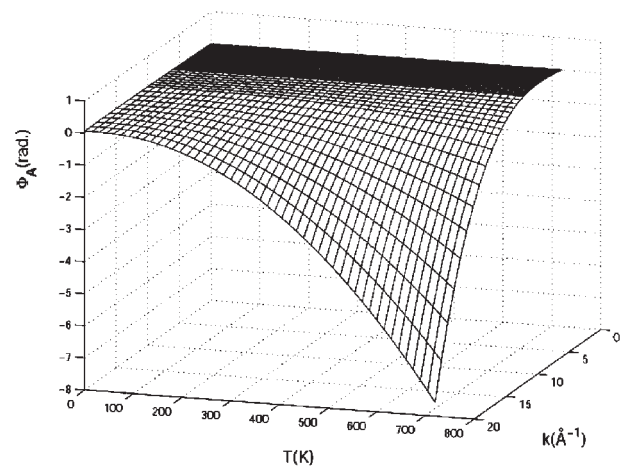


Fig. 6. Temperature and k -dependence of the calculated anharmonic contribution $\Phi_A(t, k)$ to the EXAFS phase of Cu.

previous prediction^{11,12)} and with experiment.^{2,17)} Therefore, σ_A^2 also makes it possible to determine the temperature above which the anharmonic effects or the phonon-phonon interaction are visible. For Cu this temperature is about 100 K. The increase of the anharmonic contribution to the EXAFS amplitude at high temperature characterizes the attenuation of EXAFS spectra in comparison to the one calculated by the harmonic model (Fig. 7). Figure 3 illustrates the temperature dependence of our calculated total MSRD $\sigma^2(T)$ of Cu compared to its harmonic one $\sigma_H^2(T)$ and to the experiment.^{17,19)} The difference between the total and the harmonic values becomes visible at 100 K, but it is very small and can be important only from about room temperature. Our calculated value $8.67 \times 10^{-3} \text{ \AA}^2$ of the total anharmonic MSRD at 295 K agree well with the measured one^{17,19)} of $8.67 \times 10^{-3} \text{ \AA}^2$ and with other theory¹⁴⁾ result of $5.20 \times 10^{-3} \text{ \AA}^2$. Our result at 700 K also agrees well with experiment.¹⁹⁾ The temperature dependence of the calculated first cumulant $\sigma^{(1)}$ and third cumulant $\sigma^{(3)}$ of Cu are illustrated in Figs. 4 and 5, respectively. They contribute to the phase shifts of the EXAFS due to anharmonicity (Fig. 6). Theoretical results agree well with the experimental values at 295 K for $\sigma^{(1)}$ ¹⁹⁾ and for $\sigma^{(3)}$.^{17,19)} Figure 6 illustrates the temperature and k -dependence of our calculated anharmonic contribution $\Phi_A(k, T)$ to the EXAFS phase of Cu for the first

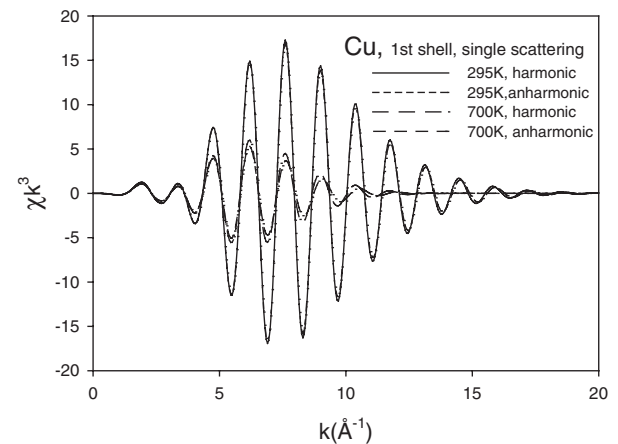


Fig. 7. Comparison of the calculated EXAFS spectrum of Cu at 295 K and 700 K including the anharmonic contribution to the one calculated by the harmonic model for the first shell for single scattering.

shell for single scattering. These contributions are especially large at high temperatures and high k -values. They contribute to the phase differences between the calculated anharmonic EXAFS spectra at different high temperatures and to their phase shifts compared to those calculated by the harmonic model. Figure 7 shows the difference between the

EXAFS spectra χk^3 of Cu at 295 K and 700 K calculated by the harmonic FEFF code¹⁾ and those including anharmonic contributions. The anharmonic spectra are shifted to the left and attenuated especially at high k-values. Fourier transform magnitudes over the range $2.5 \text{ \AA}^{-1} < k < 13 \text{ \AA}^{-1}$ for $T = 297 \text{ K}$ [Fig. 8(a)] and for $T = 703 \text{ K}$ [Fig. 8(b)] of EXAFS spectra of Cu calculated by the present anharmonic theory are compared to those calculated by the harmonic FEFF code¹⁾ and to the experimental results,¹⁹⁾ measured at HASYLAB (DESY, Germany). For XANES the multiple scattering is important, but for EXAFS the single scattering is dominant,²⁶⁾ and the main contribution to EXAFS is given by the first shell.⁷⁾ This is why for testing the theory only the calculated EXAFS of the first shell for single scattering has been used for the comparison to the experiment. The generalization to the other shells is straightforward. Our calculated EXAFS Fourier transform magnitudes of Cu including anharmonic contributions for the first shell agree well with the measured ones. They are shifted to smaller distances by 0.03 \AA at 297 K and by 0.07 \AA at 703 K in

comparison to the harmonic model results, as well as yielding apparently different structural information at the different high temperatures.

4. Conclusion

A new analytical procedure for calculation and analysis of EXAFS and its parameters including anharmonic contributions has been developed based on the cumulant expansion and the single-shell model. Our development is the derivation of the expressions for the anharmonic contributions to the amplitude and to the phase of the EXAFS. Total MSRD is the sum of the harmonic and the anharmonic ones. The anharmonic contribution to the MSRD is obtained by multiplication of the harmonic MSRD with the new derived anharmonic factor which characterizes anharmonic contribution to the EXAFS amplitude.

Anharmonic contributions to the EXAFS and its parameters such as amplitude, phase, Fourier transform magnitude and the cumulants can be calculated and analyzed for any temperature and for any k-value. The expressions derived for the EXAFS and its parameters include anharmonic contributions at high temperatures and are approaching those of the harmonic model at low temperature. Moreover, based on the anharmonic contribution to the EXAFS amplitude we also can predict the temperature above which the anharmonicity or the phonon-phonon interaction in the EXAFS is visible. Therefore, this work not only shows the advantages of the analytical procedure towards the ab initio calculation of the EXAFS and its parameters including anharmonic contributions, but also provides more useful and suggesting information compared to the previous empirical procedure.

Based on the anharmonic correlated Einstein model the calculating procedure is simplified yet provides a good agreement of the calculated results for Cu with experiment. This denotes the advantage and efficiency of the present procedure for calculation and analysis of the EXAFS and its parameters including anharmonic contributions.

Acknowledgements

One of the authors (N.V.H.) thanks the BUGH Wuppertal for financial support and hospitality. The authors thank Professor J. J. Rehr for very helpful comments and for reading the manuscript of the paper before submission and Dr. L. Tröger for providing the data of high temperature EXAFS of Cu. Useful discussions with Dr. D. Lützenkirchen-Hecht are gratefully acknowledged.

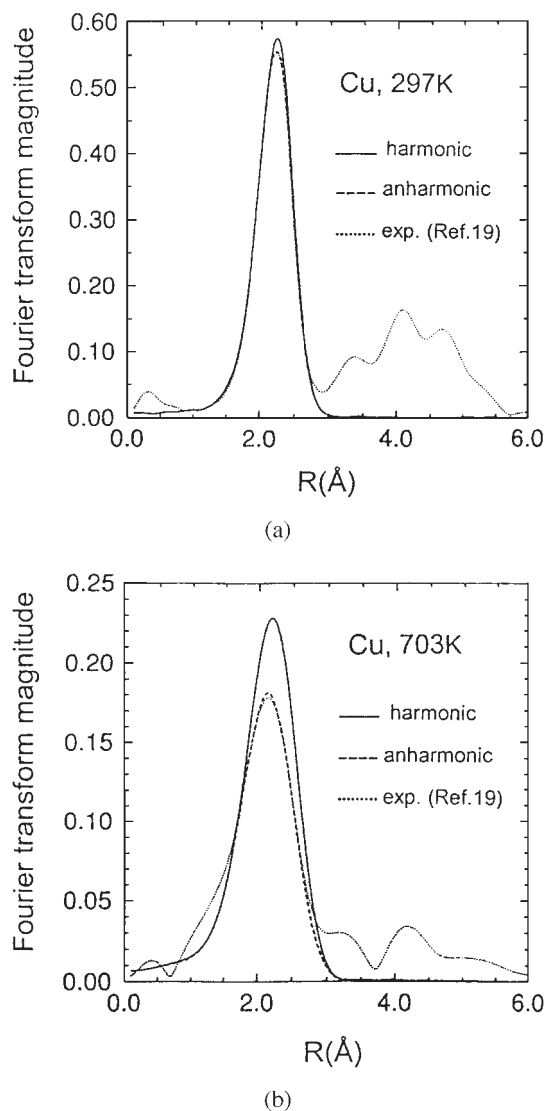


Fig. 8. Comparison of the Fourier transform magnitude of EXAFS spectrum of Cu for the first shell for single scattering calculated by the present anharmonic theory to those of the harmonic model¹⁾ and of the experiment¹⁹⁾ for $T = 297 \text{ K}$ (a) and $T = 703 \text{ K}$ (b).

- 1) J. J. Rehr, J. Mustre de Leon, S. I. Zabinsky and R. C. Albers: *J. Am. Chem. Soc.* **113** (1991) 5135.
- 2) B. S. Clausen, L. Grabæk, H. Topsøe, L. B. Hansen, P. Stoltze, J. K. Nørskov and O. H. Nielsen: *J. Catal.* **141** (1993) 368.
- 3) E. D. Crozier, J. J. Rehr and R. Ingalls: *X-ray absorption*, ed. D. C. Koningsberger and R. Prins (Wiley, New York, 1988) Chap. 9.
- 4) J. M. Tranquada and R. Ingalls: *Phys. Rev. B* **28** (1983) 3520.
- 5) G. Bunker: *Nucl. Instrum. Methods* **207** (1983) 437.
- 6) L. Wenzel, D. Arvanitis, H. Rabus, T. Lederer and L. Baberschke: *Phys. Rev. Lett.* **64** (1990) 1765.
- 7) E. A. Stern, P. Livins and Z. Zhang: *Phys. Rev. B* **43** (1991) 8850.
- 8) E. Burattini, G. Dalba, D. Diop, P. Fornasini and F. Rocca: *Jpn. J. Appl. Phys.* **32** (1993) 90; P. Fornasini, F. Monti and A. Sanson: *J. Synchrotron Radiat.* **8** (2001) 1214.

- 9) L. Tröger, T. Yokoyama, D. Arvanitis, T. Lederer, M. Tischer and K. Baberschke: Phys. Rev. B **49** (1994) 888.
- 10) N. V. Hung and R. Frahm: Physica B **208 & 209** (1995) 91.
- 11) N. V. Hung, R. Frahm and H. Kamitsubo: J. Phys. Soc. Jpn. **65** (1996) 3571.
- 12) N. V. Hung: J. Phys. IV (Paris) (1997) C2-279.
- 13) A. I. Frenkel and J. J. Rehr: Phys. Rev. B **48** (1993) 585.
- 14) T. Miyanaga and T. Fujikawa: J. Phys. Soc. Jpn. **63** (1994) 1036; *ibid.* **63** (1994) 3683.
- 15) N. V. Hung and J. J. Rehr: Phys. Rev. B **56** (1997) 43.
- 16) T. Yokoyama: Phys. Rev. B **57** (1998) 3423.
- 17) T. Yokoyama, T. Sasukawa and T. Ohta: Jpn. J. Appl. Phys. **28** (1989) 1905.
- 18) A. V. Poiarkova and J. J. Rehr: Phys. Rev. B **59** (1999) 948.
- 19) L. Tröger: unpublished.
- 20) B. T. M. Willis and A. W. Pryor: *Thermal Vibrations in Crystallography* (Cambridge University Press, London, 1975).
- 21) E. C. Marques, D. R. Sandrom, F. W. Lytle and R. B. Gregor: J. Chem. Phys. **77** (1982) 1027.
- 22) *Introduction to Solid State Physics*, ed. C. Kittel (John Wiley & Sons, New York 1986).
- 23) L. A. Girifalco and V. G. Weizer: Phys. Rev. **114** (1959) 687.
- 24) N. V. Hung and D. X. Viet: unpublished.
- 25) G. Dalba and P. Fornasini: unpublished.
- 26) P. Rennert and N. V. Hung: Phys. Status Solidi B **148** (1988) 49.
- 27) I. V. Pirog, T. I. Nedoseikina, I. A. Zarubin and A. T. Shuvaev: J. Phys.: Condens. Matter **14** (2002) 1825.
- 28) M. Daniel, D. M. Pease and J. I. Budnick: submitted to Phys. Rev. B.
- 29) J. J. Rehr and R. C. Albers: Rev. Mod. Phys. **72** (2000) 621.